Pricing Discrete Timer Options under Stochastic Volatility Models

Yue Kuen KWOK

Department of Mathematics
Hong Kong University of Science and Technology
Hong Kong

* This is a joint work with Pingping Zeng and Wendong Zheng.

Agenda

1. Product nature and uses of timer options
    - Barrier options in the volatility space: knock-out depends on the discrete realized variance hitting the preset variance budget
    - Hedge downside risk with timing uncertainty
    - Capture volatility premium

2. Analytic pricing of timer options under the stochastic volatility 3/2-model
    - Decomposition into a portfolio of timerlets
    - Joint characteristic function of log-asset price and integrated variance

3. Numerical pricing of timer options using the Hilbert transform algorithm

   - The Fourier transform of a function multiplied by an indicator function (barrier feature) is related to the Hilbert transform of the Fourier transform: avoidance of nuisance of moving between the real space and Fourier space to check the knock-out condition

   - Evaluation via the Sinc expansion: exponential decay of the truncation errors

Volatility misspecification risk

- The level of implied volatility is often higher than the realized volatility, reflecting the risk premium due to uncertainty of the future asset price movement.

- As revealed by empirical studies, 80% of the three-month calls that have matured in-the-money were overpriced.

- In a timer option, we fix volatility and allow maturity to float. This would resolve the volatility misspecification risk.

Variance budget

At initiation of the timer option, the investor specifies an expected investment horizon T and a target volatility σ_0 to define a *variance budget*

$$B = \sigma_0^2 T.$$

Let t_i, $i = 0, 1, 2, \ldots, N$, be the monitoring dates. Let τ_B be the first time in the tenor of monitoring dates at which the discrete realized variance exceeds the variance budget B, namely,

$$\tau_B = \min\left\{ j \left| \sum_{i=1}^{j} \left(\ln \frac{S_{t_i}}{S_{t_{i-1}}} \right)^2 \geq B \right. \right\} \Delta.$$

Here, Δ is the time interval between consecutive monitoring dates.

Termination date of a finite-maturity timer option $= \min(\tau_B, T)$, where T is the preset *mandated* expiration date.

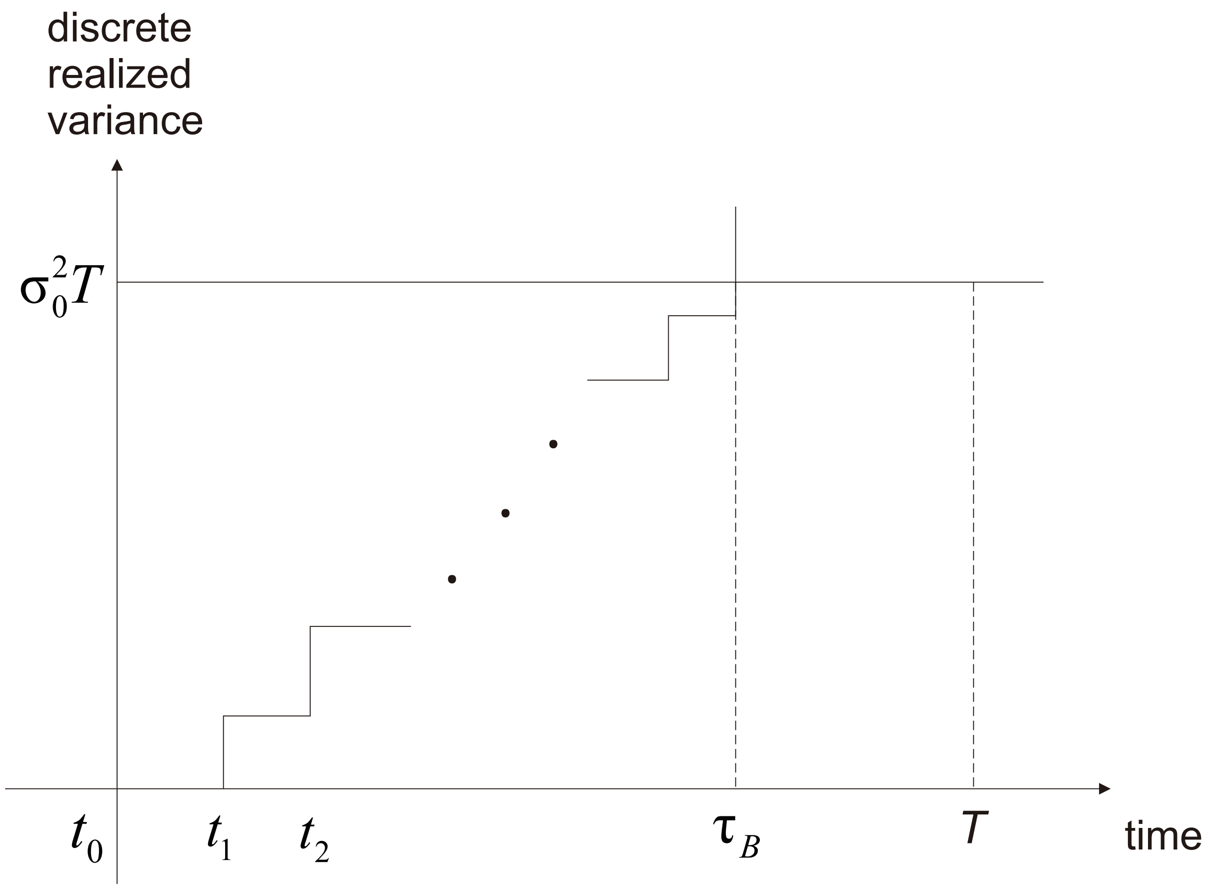

Knocked out at τ_B, which is earlier than T

Uses of timer options

- Portfolio managers can use timer put options on an index to hedge their downside risk due to sudden market drops (*with uncertainty in timing*). Cashflows from the timer put payoff are received right after the incidence of market drop.

- If one feels the implied volatility in the market is too high currently, then one can *capture the volatility risk* premium by longing a timer call and short a vanilla call. The volatility target is set below the current implied volatility and the volatility risk is captured by the difference in time value of the two options.

Analytic pricing of discretely monitored finite-maturity timer options under the stochastic volatility 3/2-model

Define the continuous integrated variance (quadratic variation) to be $I_t = \int_0^t V_s \, ds$. We use I_t as a proxy of the discrete realized variance for the monitoring of the first hitting time. We define τ_B to be

$$\tau_B = \min\left\{ j \middle| I_{t_j} \geq B \right\} \Delta.$$

This approximation does not introduce a noticeable error for daily monitored timer options. Note that

$$\begin{aligned} C_0(X_0, I_0, V_0) &= \mathbb{E}_0[e^{-r(T\wedge\tau_B)} \max(S_{T\wedge\tau_B} - K, 0)] \\ &= \mathbb{E}_0[e^{-rT} \max(S_T - K, 0)\mathbf{1}_{\{\tau_B > T\}} \\ &\quad + e^{-r\tau_B} \max(S_{\tau_B} - K, 0)\mathbf{1}_{\{\tau_B \leq T\}}], \end{aligned}$$

where K is the strike price and r is the constant interest rate.

Decomposition into a portfolio of timerlets

The event $\{\tau_B > t\}$ is equivalent to $\{I_t < B\}$. Note that $\tau_B = t_{j+1}$ if and only if $I_{t_j} < B$ and $I_{t_{j+1}} \geq B$. Therefore, we have

$$\{\tau_B \leq T\} = \bigcup_{j=0}^{N-1} \{I_{t_j} < B, I_{t_{j+1}} \geq B\}.$$

The price of a *finite-maturity discrete* timer call option can be conveniently computed by decomposing it into a portfolio of timerlets as follows

$$\begin{aligned} C_0 = {} & \mathbb{E}_0[\,e^{-rT}\max(S_T - K, 0)\mathbf{1}_{\{I_T<B\}}] \\ & + \ \mathbb{E}_0\left[\sum_{j=0}^{N-1} e^{-rt_{j+1}}\left(\max(S_{t_{j+1}} - K, 0)\mathbf{1}_{\{I_{t_j}<B\}}\right.\right. \\ & \left.\left. - \ \max(S_{t_{j+1}} - K, 0)\mathbf{1}_{\{I_{t_{j+1}}<B\}}\right)\right]. \end{aligned}$$

The challenge is the modeling of the joint processes of $\{S_{t_{j+1}}, I_{t_j}\}$ and $\{S_{t_{j+1}}, I_{t_{j+1}}\}$.

The 3/2 stochastic volatility model

Consider the 3/2 stochastic volatility model specified as follows:

$$\frac{\mathrm{d}S_t}{S_t} = (r-q)\mathrm{d}t + \sqrt{V_t}\Big(\rho\,\mathrm{d}W_t^1 + \sqrt{1-\rho^2}\,\mathrm{d}W_t^2\Big),$$
$$\mathrm{d}V_t = V_t(\theta_t - \kappa V_t)\mathrm{d}t + \varepsilon V_t^{3/2}\mathrm{d}W_t^2,$$

where W_t^1 and W_t^2 are two independent Brownian motions.

- The speed of mean reversion is now κV_t, which is linear in V_t. The mean reversion is faster when the instantaneous variance is higher.

- The parameter ε cannot be interpreted as the same volatility of variance in the Heston model.

Partial Fourier transform of the triple joint density function under 3/2 model

Write log asset price $X_t = \ln S_t$ and integrated variance $I_t = \int_0^t V_s \, \mathrm{d}s$, where I_t is used as a proxy for the discrete realized variance used in the barrier condition in the timer option.

Let $G(t, x, y, v; t', x', y', v')$ be the joint transition density of the triple (X, I, V) from state (x, y, v) at time t to state (x', y', v') at a later time t'.

The joint transition density G satisfies the following three-dimensional Kolmogorov backward equation:

$$-\frac{\partial G}{\partial t} = \left(r - q - \frac{v}{2}\right)\frac{\partial G}{\partial x} + \frac{v}{2}\frac{\partial^2 G}{\partial x^2} + v\frac{\partial G}{\partial y} + v(\theta_t - \kappa v)\frac{\partial G}{\partial v} + \frac{\varepsilon^2 v^3}{2}\frac{\partial^2 G}{\partial v^2} + \rho\varepsilon v^2 \frac{\partial^2 G}{\partial x \partial v},$$

with the terminal condition:

$$G(t', x, y, v; t', x', y', v') = \delta(x - x')\delta(y - y')\delta(v - v'),$$

where $\delta(\cdot)$ is the Dirac delta function.

We define the *generalized partial Fourier transform* of G by $\check{G}$ as follows:

$$\check{G}(t,x,y,v;t',\omega,\eta,v') = \int_{-\infty}^{\infty}\int_{0}^{\infty} e^{\mathrm{i}\omega x'+\mathrm{i}\eta y'} G(t,x,y,v;t',x',y',v')\mathrm{d}y'\mathrm{d}x',$$

where the transform variables ω and η are complex variables. The partial transform $\check{G}$ also solves the above three-dimensional Kolmogorov equation with the terminal condition: $\check{G}(t',x,y,v;t',\omega,\eta,v') = e^{\mathrm{i}\omega x+\mathrm{i}\eta y}\delta(v-v')$.

Note that $\check{G}$ admits the following solution form:

$$\check{G}(t,x,y,v;t',\omega,\eta,v') = e^{\mathrm{i}\omega x+\mathrm{i}\eta y} g(t,v;t',\omega,\eta,v'),$$

where g satisfies the following one-dimensional partial differential equation:

$$-\frac{\partial g}{\partial t} = \left[\mathrm{i}\omega\left(r-q-\frac{v}{2}\right)-\omega^2\frac{v}{2}+\mathrm{i}\eta v\right]g+[v(\theta_t-\kappa v)+\mathrm{i}\omega\rho\varepsilon v^2]\frac{\partial g}{\partial v}+\frac{\varepsilon^2 v^3}{2}\frac{\partial^2 g}{\partial v^2},$$

with the terminal condition:

$$g(t',v;t',\omega,\eta,v') = \delta(v-v').$$

The double generalized Fourier transform on the log-asset and integrated variance pair reduces the three-dimensional governing equation to a one-dimensional equation.

We manage to obtain

$$
\begin{aligned}
& g(t, v; t', v') \\
= \; & e^{a(t'-t)} \frac{A_t}{C_t} \exp\left(-\frac{A_t v + v'}{C_t v v'}\right) (v')^{-2} \left(\frac{A_t v}{v'}\right)^{\frac{1}{2}+\frac{\tilde{\kappa}}{\varepsilon^2}} I_{2c}\left(\frac{2}{C_t}\sqrt{\frac{A_t}{v v'}}\right),
\end{aligned}
$$

where I_{2c} is the modified Bessel function of order $2c$,

$$
\begin{aligned}
& a = \mathrm{i}\omega(r-q), \quad \tilde{\kappa} = \kappa - \mathrm{i}\omega\rho\varepsilon, \quad A_t = e^{\int_t^{t'} \theta_s \, \mathrm{d}s}, \\
& C_t = \frac{\varepsilon^2}{2} \int_t^{t'} e^{\int_t^s \theta_{s'} \mathrm{d}s'} \mathrm{d}s, \quad c = \sqrt{\left(\frac{1}{2} + \frac{\tilde{\kappa}}{\varepsilon^2}\right)^2 + \frac{\mathrm{i}\omega + \omega^2 - 2\mathrm{i}\eta}{\varepsilon^2}}.
\end{aligned}
$$

Note that c is in general complex and the numerical valuation of a modified Bessel function of complex order may pose some numerical challenge.

Solution procedure for obtaining $g(t, v; t', v')$

The reciprocal of the 3/2 process is a CIR process. Indeed, if we define $U_t = \dfrac{1}{V_t}$, then U_t is governed by

$$dU_t = [(\kappa + \epsilon^2) - \theta_t U_t]dt - \epsilon\sqrt{U_t}dW_t.$$

For any $t' > t$, $U_{t'}$ follows a non-central chi-square distribution conditional on U_t. The corresponding (conditional) density function is given by

$$p_U(U_{t'}|U_t) = \frac{A_t}{C_t}\exp\left(-\frac{A_t U_{t'} + U_t}{C_t}\right)\left(\frac{A_t U_{t'}}{U_t}\right)^{\frac{1}{2}+\frac{\kappa}{\epsilon^2}} I_{1+\frac{2\kappa}{\epsilon^2}}\left(\frac{2}{C_t}\sqrt{A_t U_{t'} U_t}\right).$$

Evaluation of the timelets

To evaluate the series of expectations in the portfolio of timerlets, we derive the explicit representation for the characteristic functions of (X_{t_j}, I_{t_j}) and $(X_{t_{j+1}}, I_{t_j})$.

The characteristic function of (X_{t_j}, I_{t_j}) is found to be

$$\mathbb{E}_0[e^{\mathrm{i}\omega X_{t_j}+\mathrm{i}\eta I_{t_j}}] = e^{\mathrm{i}\omega X_0+\mathrm{i}\eta I_0} h(t_0, V_0; t_j, \omega, \eta),$$

where

$$\begin{aligned} h(t, v; t', \omega, \eta) &= \int_0^\infty g(t, V_t; t', \omega, \eta, v')\ dv' \\ &= e^{a(t'-t)} \frac{\Gamma(\tilde{\beta}-\tilde{\alpha})}{\Gamma(\tilde{\beta})} \left(\frac{1}{C_t v}\right)^{\tilde{\alpha}} M\left(\tilde{\alpha}, \tilde{\beta}, -\frac{1}{C_t v}\right), \end{aligned}$$

$$\tilde{\alpha} = -\frac{1}{2} - \frac{\tilde{\kappa}}{\varepsilon^2} + c, \quad \tilde{\beta} = 1 + 2c,$$

Γ is the gamma function, M is the confluent hypergeometric function of the first kind.

Joint characteristic function of I_t and S_t across two successive time points

The expectation calculation

$$\mathbb{E}_0[e^{-rt_{j+1}}\max(S_{t_{j+1}} - K, 0)\mathbf{1}_{\{I_{t_j<B}\}}]$$

requires the joint characteristic function of I_t at t_j and S_t at t_{j+1}.

By virtue of a two-step expectation calculation, we obtain

$$\begin{aligned} & \mathbb{E}_0[e^{i\omega X_{t_{j+1}} + i\eta I_{t_j}}] \\ = \quad & e^{i\omega X_0 + i\eta I_0} \int_0^\infty g(t_0, V_0; t_j, \omega, \eta, v') h(t_j, v'; t_{j+1}, \omega, 0)\ dv'. \end{aligned}$$

Here, v' is the dummy variable for the instantaneous variance V_{t_j}.

Iterated expectation

Working backward in time from t_{j+1} to t_j, we compute $E_{t_j}[e^{i\omega X_{t_{j+1}}}]$; and from t_j to t_0, we compute $E_0[e^{i\omega X_{t_j}+i\eta I_{t_j}}]$. This is done by setting $\eta = 0$ in $h(t_j, v'; t_{j+1}, \omega, 0)$ and integrating over v' from 0 to ∞.

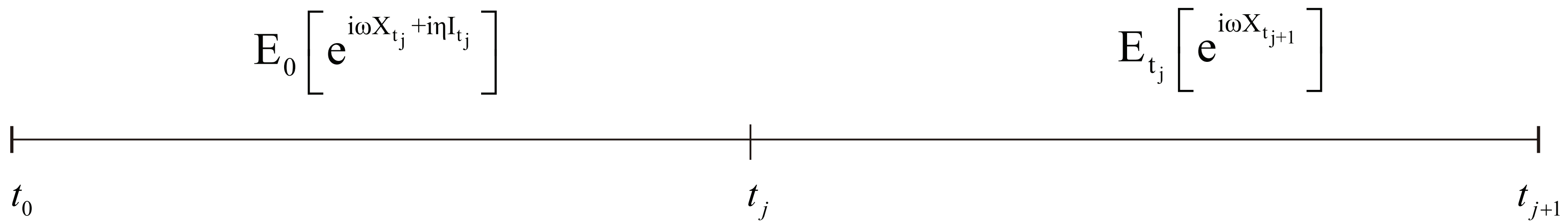

Evaluation of expectation in the Fourier domain

We transform the product of the terminal payoff and transition density function from the real domain to the Fourier domain via Parseval's theorem.

One-dimensional Parseval theorem

$$< f, g > = \int_{-\infty}^{\infty} f(x)\overline{g}(x)\ dx = \frac{1}{2\pi} < \mathcal{F}_f(u), \mathcal{F}_g(u) >$$

In the one-dimensional option pricing formulation, we may visualize $f(x)g(x)$ as the product of the density function and terminal payoff while $\mathcal{F}_f(u)\mathcal{F}_g(u)$ as the product of the characteristic function and Fourier transform of the terminal payoff.

Note that the pricing of the timerlets involves the joint process of S_t and I_t (may or may not be at the same time point).

The Fourier transform of the terminal payoff $(S_{t_{j+1}} - K, 0)\mathbf{1}_{\{I_{t_j}<B\}}$ and $(S_{t_{j+1}} - K, 0)\mathbf{1}_{\{I_{t_{j+1}}<B\}}$ admit the same analytic representation

$$\widehat{F}(\omega, \eta) = \int_{-\infty}^{\infty}\int_{-\infty}^{\infty} e^{-\mathrm{i}\omega x - \mathrm{i}\eta y}(e^x - K)^+ \mathbf{1}_{\{y<B\}}\, \mathrm{d}x\mathrm{d}y = \frac{K^{1-\mathrm{i}\omega} e^{-\mathrm{i}\eta B}}{(\mathrm{i}\omega + \omega^2)\mathrm{i}\eta},$$

where x stands for $\ln S_{t_{j+1}}$ and y stands for I_{t_j} or $I_{t_{j+1}}$.

We take $\omega = \omega_R + i\omega_I$ and $\eta = \eta_R + i\eta_I$, where $\omega_I < -1$ and $\eta_I > 0$, to ensure the existence of the two-dimensional Fourier transform.

The finite-maturity discrete timer option price can be derived as

$$C_0 = \frac{1}{4\pi^2}\int_{-\infty}^{\infty}\int_{-\infty}^{\infty} e^{-rT}\widehat{F}(\omega,\eta)\mathbb{E}_0[e^{\mathrm{i}\omega X_{t_N}+\mathrm{i}\eta I_{t_N}}]\ \mathrm{d}\omega_R \mathrm{d}\eta_R$$

$$+\sum_{j=0}^{N-1}\frac{1}{4\pi^2}\int_{-\infty}^{\infty}\int_{-\infty}^{\infty} e^{-rt_{j+1}}$$

$$\left(\widehat{F}(\omega,\eta)\mathbb{E}_0[e^{\mathrm{i}\omega X_{t_{j+1}}+\mathrm{i}\eta I_{t_j}}]-\widehat{F}(\omega,\eta)\mathbb{E}_0[e^{\mathrm{i}\omega X_{t_{j+1}}+\mathrm{i}\eta I_{t_{j+1}}}]\right)\ \mathrm{d}\omega_R \mathrm{d}\eta_R$$

$$= \frac{1}{4\pi^2}\int_{-\infty}^{\infty}\int_{-\infty}^{\infty}\widehat{F}(\omega,\eta)H(\omega,\eta)\,\mathrm{d}\omega_R \mathrm{d}\eta_R,$$

where

$$H(\omega,\eta) = e^{-rT}e^{i\omega X_0+i\eta I_0}h(t_0,V_0;t_N,\omega,\eta)+e^{\mathrm{i}\omega X_0+\mathrm{i}\eta I_0}\sum_{j=0}^{N-1}e^{-rt_{j+1}}$$

$$\left[\int_0^{\infty} g(t_0,V_0;t_j,\omega,\eta,v')h(t_j,v';t_{j+1},\omega,0)\ \mathrm{d}v' - h(t_0,V_0;t_{j+1},\omega,\eta)\right].$$

Numerical challenge: Three-dimensional numerical integration is required and the integrands involve the hypergeometric functions with order that is complex.

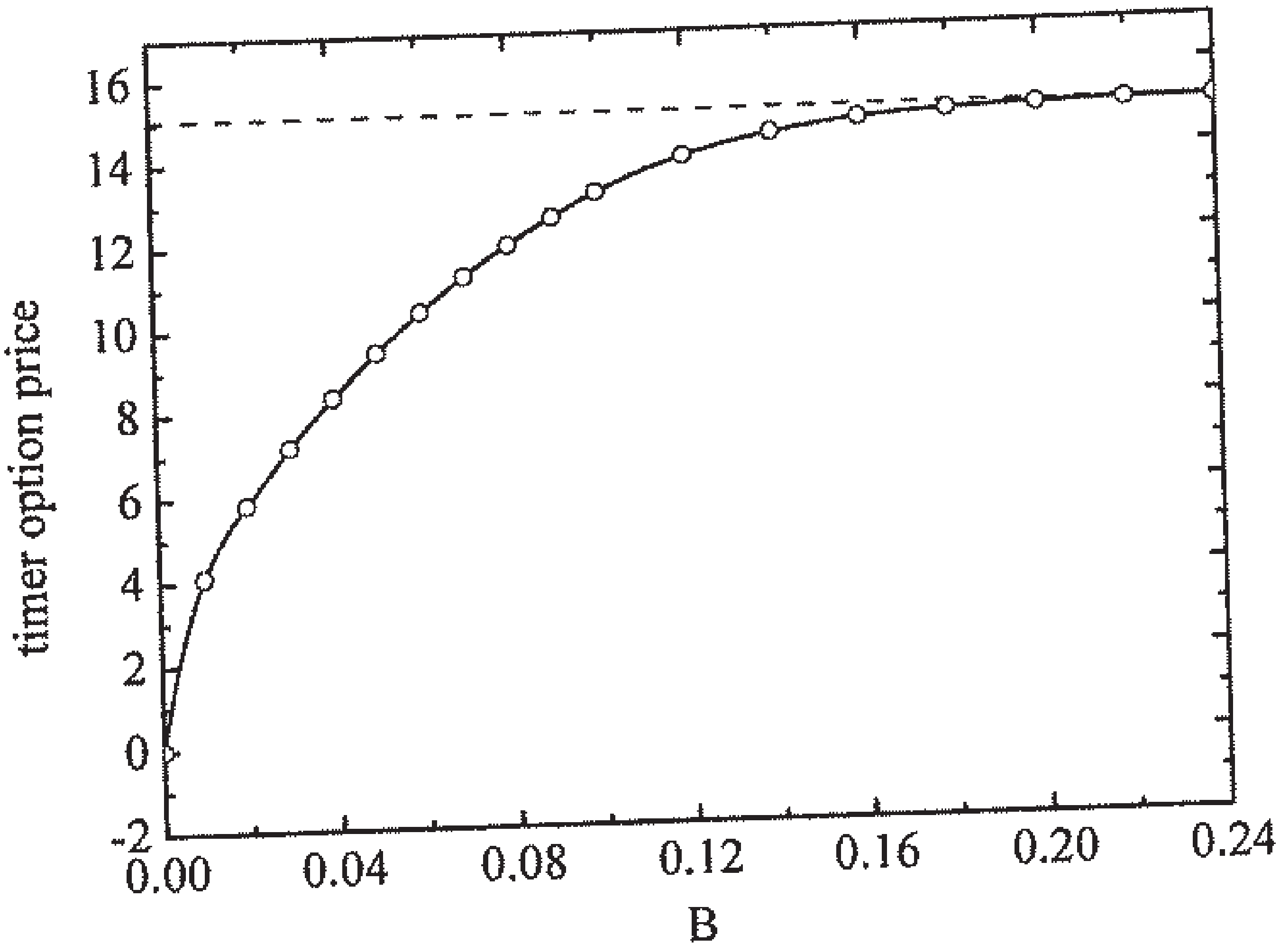

Plot of the finite-maturity discrete timer call option prices against variance budget B. The discrete timer call option price tends to that of the vanilla European call option (shown in the dashed line) when B is sufficiently large.

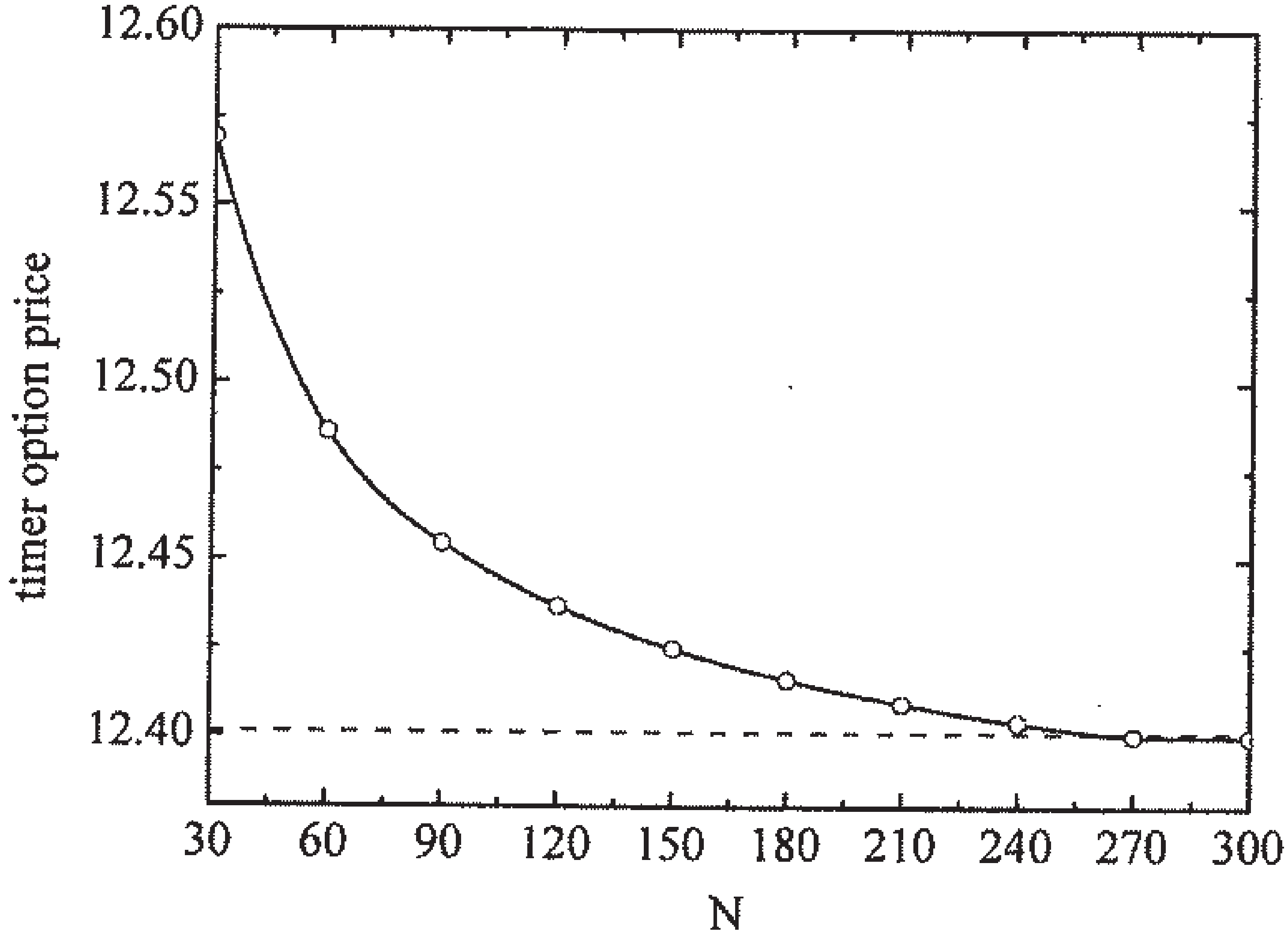

Plot of the finite-maturity discrete timer call option prices against number of monitoring instants N. The dashed line represents the finite-maturity timer call option price under continuous monitoring.

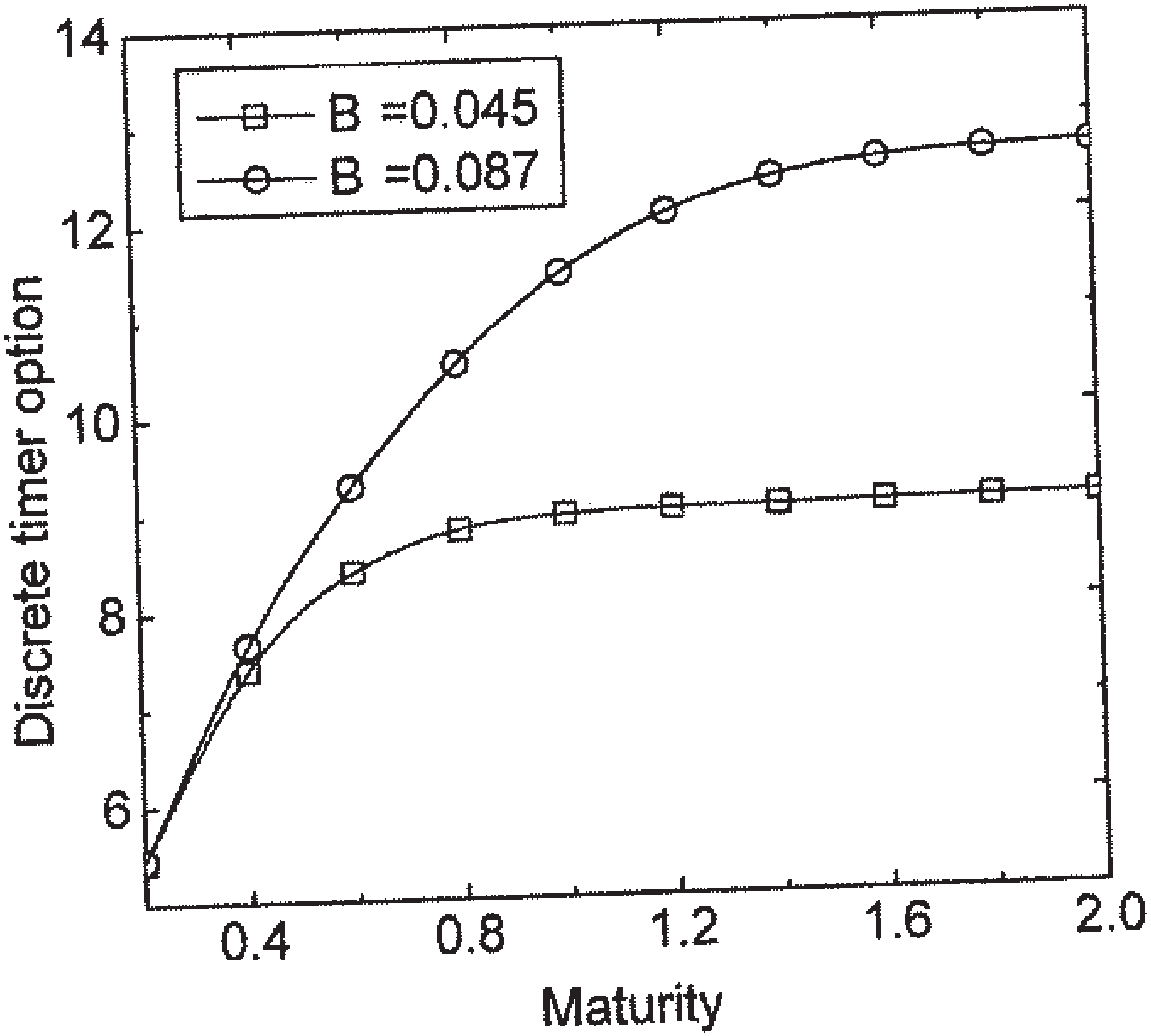

Plot of the finite-maturity discrete timer call option price versus maturity (mandated) under two different values of the variance budget.

Hilbert transform algorithm

The underlying asset price process S_t and its instantaneous variance v_t under a risk neutral measure Q are assumed to follow the following general stochastic volatility model

$$\begin{aligned}\frac{\mathrm{d}S_t}{S_t} &= (r-q)\ \mathrm{d}t + \sqrt{v_t}\ \mathrm{d}W_t^S,\\ \mathrm{d}v_t &= \alpha(v_t)\ \mathrm{d}t + \beta(v_t)\ \mathrm{d}W_t^v,\end{aligned}$$

where $E_t[\mathrm{d}W_t^S \mathrm{d}W_t^v] = \rho\ \mathrm{d}t$. Here, ρ is the correlation coefficient between the pair of Brownian motions, q is the dividend yield, the drift function $\alpha(v_t)$ and the volatility function $\beta(v_t)$ are measurable functions with respect to the natural filtration generated by the two correlated Brownian motions.

We define the continuous realized variance over $[0, t]$ by

$$I_t = \int_0^t v_s\ \mathrm{d}s.$$

Choice of log-variance as the state variable

We define $\gamma_t = \ln V_t$, $x_t = \ln \dfrac{S_t}{K}$, where K is the strike price, Δ be the uniform time interval between successive monitoring instants.

We choose the log-variance instead of variance as the state variable since the corresponding form of conditional density exhibits two advantages.

- The left tail of the conditional density of log-variance decays to zero more rapidly.

- The conditional densities of the log-variance processes for varying parameter values are more symmetric than those of the variance processes.

Value function of discrete timer call option

Let $V_{t_k}(x_{t_k}, \gamma_{t_k}, I_{t_k})$ be the option value of the finite-maturity discrete timer call option at monitoring time t_k, $k = 0, 1, \cdots, N$, where x_{t_k}, γ_{t_k} and I_{t_k} denote the time-t_k normalized log-asset return, log-variance and realized variance, respectively.

Suppose we write the continuation value conditional on $\{I_k < B\}$ as

$$U_{t_k}(x_k, \gamma_k, I_k) = E_{t_k}[V_{t_{k+1}}(x_{k+1}, \gamma_{k+1}, I_{k+1})],$$

then V_{t_k} is the sum of the following two terms:

$$V_{t_k}(x_k, \gamma_k, I_k) = e^{-r\Delta} U_{t_k}(x_k, \gamma_k, I_k) \mathbf{1}_{\{I_k < B\}} + K(e^{x_k} - 1)^+ \mathbf{1}_{\{I_k \geq B\}},$$

$k = 1, 2, \cdots, N-1$.

Time-stepping calculations between successive monitoring dates

By the tower property and conditional on the log-variance process $\gamma_{t_{k+1}}$ at time t_{k+1}, it follows that

$$U_{t_k}(x_k, \gamma_k, I_k) = E\left[E[V_{t_{k+1}}(x_{k+1}, \gamma_{k+1}, I_{k+1})|\mathcal{F}_{t_k}, \gamma_{k+1}]|\mathcal{F}_{t_k}\right].$$

The outer expectation integral involves integration over the density function $p_\gamma(\gamma_{t_{k+1}}|\gamma_{t_k})$, which has analytic closed form under the Heston and 3/2 stochastic volatility models.

- To evaluate the above three-dimensional expectation integral, we apply an interpolation based quadrature rule for the outer one-dimensional expectation integral and the Fourier transform method for the inner two-dimensional expectation integral.

- Across a monitoring date, as exemplified by the barrier condition, we can take advantage of the fast Hilbert transform method to deal with the barrier feature associated with the accumulated realized variance.

FFT technique

We adopt the numerical quadrature rule to calculate the outer expectation integral. By performing discretization along the dimension of log-variance $\gamma_{t_{k+1}}$ at the discrete nodes $\zeta_j,\ j = 1, 2, \cdots, J$, we obtain

$$U_{t_k}(x_k, \gamma_k, I_k) \approx \sum_{j=1}^{J} w_j p_\gamma(\zeta_j|\gamma_k) E\left[V_{t_{k+1}}(x_{k+1}, \gamma_{k+1}, I_{k+1})|\mathcal{F}_{t_k}, \gamma_{k+1} = \zeta_j\right],$$

where w_j is the weight at the quadrature node $\zeta_j,\ j = 1, 2, \cdots, J$.

Since only the joint conditional characteristic function of x_{k+1} and I_{k+1} is known, we apply the Fourier transform method to perform the inner expectation calculations. To guarantee that the Fourier transforms are well defined, we need to introduce a proper exponential damping factor.

Let $w = \alpha_1 + i\beta_1$ and $u = \alpha_2 + i\beta_2$, where α_1 and α_2 are constants. At $\gamma_{t_{k+1}} = \zeta_j$, $x_{t_{k+1}} = x$ and $I_{t_{k+1}} = y$, we define

$$V_{t_{k+1}}^{\alpha_1,\alpha_2}(x, \zeta_j, y) = e^{\alpha_1 x + \alpha_2 y} V_{t_{k+1}}(x, \zeta_j, y).$$

The parameters α_1, α_2 are chosen to insure the existence of the generalized two-dimensional Fourier transform of $V_{t_{k+1}}(x, \zeta_j, y)$ as defined by

$$\begin{aligned}\widehat{V}_{t_{k+1}}^{\alpha_1,\alpha_2}(\zeta_j; \beta_1, \beta_2) &= \int_{-\infty}^{\infty}\int_{-\infty}^{\infty} e^{i\beta_1 x + i\beta_2 y} V_{t_{k+1}}^{\alpha_1,\alpha_2}(x, \zeta_j, y)\, \mathrm{d}x\mathrm{d}y \\ &= \int_{-\infty}^{\infty}\int_{-\infty}^{\infty} e^{wx + uy} V_{t_{k+1}}(x, \zeta_j, y)\, \mathrm{d}x\mathrm{d}y,\end{aligned}$$

where $w = \alpha_1 + i\beta_1$ and $u = \alpha_2 + i\beta_2$.

By the renowned Parseval's theorem, we can represent the inner expectation as follows

$$
\begin{aligned}
& E[V_{t_{k+1}}(x_{k+1},\gamma_{k+1},I_{k+1})|\mathcal{F}_{t_k},\gamma_{k+1}=\zeta_j] \\
= & \int_{-\infty}^{\infty}\int_{-\infty}^{\infty} V_{t_{k+1}}(x,\zeta_j,y)\, p(x,y|\mathcal{F}_{t_k},\gamma_{k+1}=\zeta_j)\,\mathrm{d}x\mathrm{d}y \\
= & \frac{1}{4\pi^2}\int_{-\infty}^{\infty}\int_{-\infty}^{\infty} \widehat{V}_{t_{k+1}}^{\alpha_1,\alpha_2}(\zeta_j;\beta_1,\beta_2)\breve{p}(w,u|\mathcal{F}_{t_k},\gamma_{k+1}=\zeta_j)\,\mathrm{d}\beta_1\mathrm{d}\beta_2.
\end{aligned}
$$

Here, $\breve{p}(w,u|\mathcal{F}_{t_k},\gamma_{k+1} = \zeta_j) = E\Big[e^{-wx_{k+1}-uy_{k+1}}|\mathcal{F}_{t_k},\gamma_{k+1} = \zeta_j\Big]$ is visualized as the generalized inverse Fourier transform of the joint conditional density function $p(x,y|\mathcal{F}_{t_k},\gamma_{k+1}=\zeta_j)$ of $x_{t_{k+1}}$ and $I_{t_{k+1}}$.

It is convenient to express $\breve{p}(w,u|\mathcal{F}_{t_k},\gamma_{k+1}=\zeta_j)$ in the following analytic representation

$$\begin{aligned}&\breve{p}(w,u|\mathcal{F}_{t_k},\gamma_{k+1}=\zeta_j)\\ =\ & e^{-wx_k-uI_k}E[e^{-w(x_{k+1}-x_k)-u(I_{k+1}-I_k)}|\mathcal{F}_{t_k},\gamma_{k+1}=\zeta_j].\end{aligned}$$

Next, we express $\breve{p}$ in terms of the conditional moment generating function $\Psi(w,u;\gamma_t,\gamma_s)=E[e^{w(x_t-x_s)+u(I_t-I_s)}|\mathcal{F}_s,\gamma_t]$. Here, we have suppress the dependency of Ψ on $t-s$ for notational convenience.

By the tower property, for $s<t$, we have

$$\begin{aligned}\Psi(w,u;\gamma_t,\gamma_s) &= E\Big[E[e^{w(x_t-x_s)+u(I_t-I_s)}|\mathcal{F}_s,\gamma_t,I_t-I_s]|\mathcal{F}_s,\gamma_t\Big]\\ &= E\Big[E[e^{w(x_t-x_s)}|\mathcal{F}_s,\gamma_t,I_t-I_s]e^{u(I_t-I_s)}|\mathcal{F}_s,\gamma_t\Big].\end{aligned}$$

We may express the inner expectation integral at $\gamma_{t_{k+1}} = \zeta_j$ by the following two-dimensional inverse Fourier transform

$$
\begin{aligned}
& E[V_{t_{k+1}}(x_{k+1}, \gamma_{k+1}, I_{k+1}) | \mathcal{F}_{t_k}, \gamma_{k+1} = \zeta_j] \\
= \quad & \frac{1}{4\pi^2} \int_{-\infty}^{\infty} \int_{-\infty}^{\infty} e^{-wx_k - uI_k} \widehat{V}_{t_{k+1}}^{\alpha_1, \alpha_2}(\zeta_j; \beta_1, \beta_2) \Psi(-w, -u; \zeta_j, \gamma_k)\, \mathrm{d}\beta_1 \mathrm{d}\beta_2.
\end{aligned}
$$

Here, we have set $\gamma_{t_{k+1}} = \zeta_j$ in the conditional moment generating function $\Psi(w, u; \gamma_{k+1}, \gamma_k)$.

Next, we show that $\Psi(w, u; \gamma_t, \gamma_s)$ possesses closed form analytic representation under the Heston model and the 3/2 stochastic volatility model via the determination of the respective kernel function.

Kernel functions for the Heston model and 3/2-model

The kernel function $\Psi(w, u; \gamma_t, \gamma_s)$ is the input that characterizes the specific stochastic volatility model. We derive the explicit representation of $\Psi(w, u; \gamma_t, \gamma_s)$ for the Heston model and 3/2 stochastic volatility model.

Under the general stochastic volatility model, the asset price process admits the following representation

$$S_t = S_0 e^{(r-q)t + a_t + \sqrt{b_t} W},$$

where a_t and b_t are defined by

$$a_t = \rho[f(v_t) - f(v_0)] - \rho H_t - \frac{I_t}{2} \quad \text{and} \quad b_t = (1 - \rho^2) I_t,$$

with

$$H_t = \int_0^t h(v_s)\ \mathrm{d}s \quad \text{and} \quad f(v_t) = \int \frac{\sqrt{v_t}}{\beta(v_t)}\ \mathrm{d}v_t.$$

Here, W is a standard normal random variable and h is defined by

$$h(v_t) = \alpha(v_t) f'(v_t) + \frac{1}{2}\beta^2(v_t) f''(v_t).$$

Heston model

For the Heston stochastic volatility model, the dynamics for its variance is defined by

$$\mathrm{d}v_t = \lambda(\bar{v} - v_t)\ \mathrm{d}t + \eta\sqrt{v_t}\ \mathrm{d}W_t^v.$$

In the Heston model, $\alpha(v_t) = \lambda(\bar{v} - v_t)$ and $\beta(v_t) = \eta\sqrt{v_t}$. It follows that $f(v_t) = \frac{v_t}{\eta}$ and $h(v_t) = \frac{\lambda(\bar{v}-v_t)}{\eta}$.

We can rewrite the normalized log-asset return process as follows

$$x_t = \ln\frac{S_0}{K} + (r-q)t + \frac{\rho}{\eta}(e^{\gamma_t} - e^{\gamma_0} - \lambda\bar{v}t) + \left(\frac{\rho\lambda}{\eta} - \frac{1}{2}\right)I_t + \sqrt{(1-\rho^2)I_t}\,W.$$

We obtain

$$
\begin{aligned}
&\Psi(w,u;\gamma_t,\gamma_s)\\
&= E\left[E[e^{w(x_t-x_s)}|\mathcal{F}_s,\gamma_t,I_t-I_s]e^{u(I_t-I_s)}|\mathcal{F}_s,\gamma_t\right]\\
&= e^{w\left\{(r-q)(t-s)+\frac{\rho}{\eta}[e^{\gamma_t}-e^{\gamma_s}-\lambda\bar{v}(t-s)]\right\}}\\
&\qquad \Phi\left(-iw\left(\frac{\rho\lambda}{\eta}-\frac{1}{2}\right)-\frac{1}{2}iw^2(1-\rho^2)-iu;e^{\gamma_t},e^{\gamma_s}\right),
\end{aligned}
$$

where

$$\Phi(\xi;\gamma_t,\gamma_s) = E[e^{i\xi\int_s^t v_u\,\mathrm{d}u}|\gamma_t,\gamma_s]$$

is the conditional characteristic function of the time-integrated log-variance process $\int_s^t v_u\,\mathrm{d}u$.

With the use of the kernel function, one can express the two-dimensional moment generating function Ψ in terms of the one-dimensional characteristic function Φ.

3/2 stochastic volatility model

The variance process evolves according to the following dynamics

$$\mathrm{d}v_t = \lambda v_t(\bar{v} - v_t)\ \mathrm{d}t + \eta v_t^{3/2}\ \mathrm{d}W_t^v.$$

The use of It$\hat{o}$'s formula gives the corresponding dynamics for $\frac{1}{v_t}$

$$\mathrm{d}\left(\frac{1}{v_t}\right) = \lambda\bar{v}\left(\frac{\lambda + \eta^2}{\lambda\bar{v}} - \frac{1}{v_t}\right)\ \mathrm{d}t - \frac{\eta}{\sqrt{v_t}}\ \mathrm{d}W_t^v.$$

The reciprocal of the variance process of the 3/2 model follows a mean-reverting square-root process with parameters $(\lambda\bar{v}, \frac{\lambda+\eta^2}{\lambda\bar{v}}, -\eta)$.

In this case, $\alpha(v_t) = \lambda v_t(\bar{v} - v_t)$ and $\beta(v_t) = \eta v_t^{3/2}$. It follows that $f(v_t) = \frac{\ln v_t}{\eta}$ and $h(v_t) = \frac{\lambda}{\eta}\left[\bar{v} - \left(1 + \frac{\eta^2}{2\lambda}\right)v_t\right]$.

The normalized log-asset return process can be expressed as in the following form

$$x_t = \ln \frac{S_0}{K} + (r-q)t + \frac{\rho}{\eta}\left[\gamma_t - \gamma_0 - \lambda \bar{v} t\right] + \left[\frac{\rho\lambda}{\eta}\left(1 + \frac{\eta^2}{2\lambda}\right) - \frac{1}{2}\right] I_t + \sqrt{(1-\rho^2) I_t}\, W.$$

Similarly, we have

$$\begin{aligned} &\Psi(w, u; \gamma_t, \gamma_s) \\ = \; & e^{w\left\{(r-q)(t-s) + \frac{\rho}{\eta}[\gamma_t - \gamma_s - \lambda\bar{v}(t-s)]\right\}} \\ & \Phi\left(-iw\left[\frac{\rho\lambda}{\eta}\left(1 + \frac{\eta^2}{2\lambda}\right) - \frac{1}{2}\right] - \frac{1}{2} i w^2 (1-\rho^2) - iu; e^{\gamma_t}, e^{\gamma_s}\right). \end{aligned}$$

Definition of the Hilbert transform

For any $f \in L^p(\mathbb{R}), 1 \leq p < \infty$, we define the Fourier transform $\hat{f}$ by

$$\hat{f} = \mathcal{F}f = \int_{-\infty}^{\infty} e^{i\beta x} f(x)\ \mathrm{d}x,$$

and $\widehat{f} = \mathcal{F}f \in L^q(\mathbb{R})$ with $\frac{1}{p} + \frac{1}{q} = 1$.

For any $f \in L^p(\mathbb{R}), 1 \leq p < \infty$, its Hilbert transform is defined by the Cauchy principal value integral

$$\mathcal{H}f(x) = \frac{1}{\pi} PV \int_{\mathbb{R}} \frac{f(y)}{x-y}\ \mathrm{d}y,$$

and $H\widehat{f} \in L^q(\mathbb{R})$ with $\frac{1}{p} + \frac{1}{q} = 1$.

Two key properties of the Hilbert transform

For any $b \in \mathbb{R}$, the Fourier transform of a function multiplied by an indicator function $\mathbf{1}_{(-\infty,b)}$ is related to the Hilbert transform of the Fourier transform function by

$$\mathcal{F}(\mathbf{1}_{(-\infty,b)} \cdot f)(\beta) = \frac{1}{2}\widehat{f}(\xi) - \frac{i}{2}e^{i\beta b}\mathcal{H}\Big(e^{-i\eta b}\widehat{f}(\eta)\Big)(\beta).$$

The Hilbert transform can be evaluated based on the Sinc expansion of an analytic function as follows

$$\mathcal{H}f(x) = \frac{1}{\pi}PV\int_{\mathbb{R}} \frac{f(y)}{x-y}\, \mathrm{d}y = \sum_{l=-\infty}^{\infty} f(lh)\frac{1-\cos\frac{\pi(x-lh)}{h}}{\frac{\pi(x-lh)}{h}}, \quad h > 0,$$

where h is the fixed discretization step.

Fast Hilbert transform algorithm

The backward induction procedure in the Fourier domain using the fast Hilbert transform algorithm for pricing finite-maturity discrete timer options can be formulated as follows:

(i) We initiate our time stepping calculations at maturity t_N. The generalized Fourier transform of the terminal payoff admits the analytic formula

$$\widehat{V}_{t_N}^{\alpha_1,\alpha_2}(\zeta_j;\beta_1,\beta_2) = -\frac{K}{(\alpha_1+i\beta_1)(\alpha_1+i\beta_1+1)(\alpha_2+i\beta_2)},$$

for $j = 1, 2, \cdots, N$.

Here, the constraints $\alpha_1 < -1$ and $\alpha_2 < 0$ should be observed in order to guarantee the existence of the above generalized Fourier transform.

(ii) For $k = N-1, N-2, \cdots, 1$, the numerical approximation of $\widehat{V}_{t_k}^{\alpha_1,\alpha_2}(\zeta_p;\beta_1,\beta_2)$ is recursively calculated by computing a sequence of Hilbert transforms

$$\begin{aligned}
&\widehat{V}_{t_k}^{\alpha_1,\alpha_2}(\zeta_p;\beta_1,\beta_2)\\
&= e^{-r\Delta}\left[\frac{1}{2}\widehat{U}_{t_k}^{\alpha_1,\alpha_2}(\zeta_p;\beta_1,\beta_2) - \frac{i}{2}e^{i\beta_2 B}\mathcal{H}\left(e^{-i\beta_2' B}\widehat{U}_{t_k}^{\alpha_1,\alpha_2}(\zeta_p;\beta_1,\beta_2')\right)(\beta_2)\right]\\
&\qquad - \frac{Ke^{(\alpha_2+i\beta_2)B}}{(\alpha_1+i\beta_1)(\alpha_1+i\beta_1+1)(\alpha_2+i\beta_2)},\ p = 1,2,\cdots,N.
\end{aligned}$$

(iii) We approximate $\widehat{U}_{t_k}^{\alpha_1,\alpha_2}(\zeta_p;\beta_1,\beta_2)$ using the quadrature rule

$$\widehat{U}_{t_k}^{\alpha_1,\alpha_2}(\zeta_p;\beta_1,\beta_2) \approx \sum_{j=1}^{J} w_j \widehat{V}_{t_{k+1}}^{\alpha_1,\alpha_2}(\zeta_j;\beta_1,\beta_2)\Psi(-w,-u;\zeta_j,\zeta_p).$$

(iv) For the last step where $k = 0$, the timer call option value is obtained by

$$V_{t_0}(x_0,\zeta_p,I_0) \approx \sum_{j=1}^{J} \frac{e^{-r\Delta} w_j}{4\pi^2} \int_{-\infty}^{\infty}\int_{-\infty}^{\infty} e^{-(\alpha_1+i\beta_1)x_0} e^{-(\alpha_2+i\beta_2)I_0} \widehat{V}_{t_1}^{\alpha_1,\alpha_2}(\zeta_j;\beta_1,\beta_2)\Psi(-w,-u;\zeta_j,\zeta_p)\ \mathrm{d}\beta_1 \mathrm{d}\beta_2,$$

for $p = 1, 2, \cdots, N$.

Sinc approximation

We consider the evaluation of the Hilbert transform in the following form

$$q(\beta) = \mathcal{H}\left(e^{-i\eta x}\widehat{f}(\eta)\right)(\beta),$$

and the calculation of the two-dimensional inverse Fourier transform

$$g(x_1, x_2) = \frac{1}{4\pi^2}\int_{-\infty}^{\infty}\int_{-\infty}^{\infty} e^{-i\beta_1 x_1} e^{-i\beta_2 x_2}\widehat{g}(\beta_1, \beta_2)\,\mathrm{d}\beta_1 \mathrm{d}\beta_2.$$

The Hilbert transform can be evaluated by the truncated Sinc approximation

$$q_{h,L}(\beta) = \sum_{l=-L}^{L} e^{-ilhx}\widehat{f}(lh)\frac{1-\cos\frac{\pi(\beta-lh)}{h}}{\frac{\pi(\beta-lh)}{h}}.$$

The inverse Fourier transform can be evaluated numerically by the following discretized and truncated operator:

$$g_{h_1,M,h_2,L}(x_1,x_2) = \frac{1}{4\pi^2} \sum_{m=-M}^{M} \sum_{l=-L}^{L} e^{-imh_1x_1} e^{-ilh_2x_2} \widehat{g}(mh_1, lh_2) h_1 h_2.$$

The trapezoidal sum approximation has been shown to be highly accurate, exhibiting exponentially decaying discretization errors.

Computational complexity

The overall computational complexity of the fast Hilbert transform algorithm for pricing finite-maturity discrete timer options is $O(NMJ^2L \log L)$, where N is the number of monitoring instants, M, J and L are the truncation level parameters in the log-asset dimension, log-variance dimension and realized variance dimension, respectively.

Heston model

S_0	T	r	q	B	N	λ	η	$\bar{v}$	v_0
100	1.5	0.015	0	0.087	300	2	0.375	0.09	0.087

Parameter values in the Heston model and finite-maturity discrete timer options

K	ρ	Hilbert	MC	RE(%)
90	-0.5	17.6905	17.6927	-0.0124
	0	17.5517	17.5551	-0.0194
	0.5	17.4910	17.4882	0.0160
100	-0.5	12.3996	12.4099	-0.0830
	0	12.2804	12.2909	-0.0854
	0.5	12.2647	12.2692	-0.0367
110	-0.5	8.4174	8.4313	-0.1649
	0	8.3503	8.3634	0.1566
	0.5	8.3716	8.3774	-0.0692

Comparison of the numerical results for the finite-maturity discrete timer call options for varying strike prices K and correlation values ρ obtained from the fast Hilbert transform algorithm with the benchmark results obtained using the Monte Carlo method (MC) under the Heston model.

3/2-model

S_0	T	r	q	B	N	λ	η	$\bar{v}$	v_0
100	1.5	0.015	0	0.087	200	22.84	8.56	0.218	0.087

Parameter values in the 3/2 model and finite-maturity discrete timer options

K	ρ	Hilbert	MC	RE(%)
90	-0.5	17.7155	17.7383	-0.1285
	0	17.5778	17.5892	-0.0648
	0.5	17.4923	17.5016	-0.0531
100	-0.5	12.4366	12.4594	-0.1830
	0	12.3195	12.3328	-0.1078
	0.5	12.2759	12.2856	-0.0790
110	-0.5	8.4608	8.4802	-0.2287
	0	8.3951	8.4063	-0.1332
	0.5	8.3897	8.3962	-0.0774

Comparison of the numerical results for finite-maturity discrete timer call options for varying strike prices K and correlation values ρ obtained from the fast Hilbert transform algorithm with the benchmark results obtained using the Monte Carlo method (MC) under the 3/2 stochastic volatility model.

Sensitivity analysis on volatility of variance η and correlation coefficient ρ under the Heston model

- The price function may not be a monotonically increasing function of η.

- We observe that when $\rho = -0.5$, the discrete timer call option price firstly increases and then decreases with increasing value of η.

- On the other hand, when $\rho = 0.5$, the discrete timer call option price is a decreasing function of η.

Sensitivity analysis under the Heston model

ρ	η	$K = 90$	$K = 94$	$K = 98$	$K = 102$	$K = 106$	$K = 110$
	0.15	17.6571	15.3986	13.3621	11.5434	9.9315	8.5091
-0.5	0.3	17.7028	15.4356	13.3888	11.5585	9.9342	8.4989
	0.45	17.6654	15.3651	13.2840	11.4197	9.7630	8.2986
	0.15	17.5859	15.3234	13.2845	11.4650	9.8537	8.4333
0.5	0.3	17.5453	15.2842	13.2475	11.4307	9.8226	8.4056
	0.45	17.4522	15.1898	13.1569	11.3472	9.7483	8.3413

Comparison of the numerical values for finite-maturity discrete timer call option prices with varying values of strike prices, volatility of variance and correlation coefficient under the Heston model.

Conclusion

- By decomposing a timer option into a portfolio of timerlets, we manage to price a finite-maturity timer option based on the explicit representation of the joint characteristic function of log asset price and its integrated variance. The computational time for numerical evaluation of the joint characteristic function under the 3/2-model can be quite substantially lengthy.
- Our numerical tests on pricing the finite-maturity discrete timer options under the Heston model and 3/2 model demonstrate high level of numerical accuracy and robustness of the fast Hilbert algorithm for pricing options with exotic barrier feature. The computational times required for pricing under different s-tochastic volatility models do not differ significantly.

- We manage to obtain the closed form formulas for the conditional joint characteristic function and moment generating function of log asset price x_t and integrated variance I_t.

- Hedging remains a challenge since the risk factors involve the instantaneous variance and integrated variance, besides the stock price. How to use a portfolio of stock and variance derivatives in hedging remains an open question? Note that the integrated variance determines the knock-out condition.